scientific reports

Check for updates

OPEN

Real-time monitoring of ammonia emissions from cereal crops using LoRaWAN-based sensing technology

Nyéki Anikó[1]✉, Alahmad Tarek[1], Sana Arshad[2], Gombkötő Nóra[1], Neményi Miklós[1], Morad Mirzaei[3], Szabó Szilárd[4], Endre Harsanyi[5,6], Main Al-Dalahmeh[7] & Safwan Mohammed[5,6]

This study presents a LoRaWAN-based IoT system developed for real-time monitoring of ammonia (NH_3) emissions in cereal crop fields. Sustainable agriculture increasingly demands on-farm greenhouse gas (GHG) tracking linked to environmental variables. IoT offers efficient real-time monitoring of soil NH_3 emissions and associated factors. Our research introduces a unique Field Monitoring Laboratory: a LoRaWAN-connected IoT system integrating soil, crop, and microclimate sensors to observe NH_3^+, air temperature, rainfall, humidity, soil temperature, and moisture content. The system comprises a field lab, data server, and custom dashboard with analytics capabilities. NH_3 fluxes were measured in autumn-sown cereals across three growing seasons (2020–2023). Tukey's Kramer test revealed significant ($p < 0.05$, $p < 0.001$) differences in NH_3 emissions and environmental variables between years. Highest NH_3 emissions (1.94 ppm in 2020, 1.71 ppm in 2021) coincided with elevated air (25–31 °C) and soil (21–23 °C) temperatures, and higher mean and peak rainfall (0.40–0.48 mm average; max 9–31.6 mm). Principal Component Analysis showed 65.8% variance explained by PC1 and PC2, with high loadings from temperature and soil moisture. Spearman's correlation indicated moderate positive associations ($r = 0.38–0.4$, $p < 0.05$) of NH_3 with soil moisture at 20 cm and 40 cm of soil depth, and a weak negative correlation (r = -0.16 and – 0.17) with soil temperature at 20 cm and 40 cm. The study underscores the potential of IoT technology using calibrated gas sensors and LoRaWAN for real-time NH_3 and environmental monitoring, enabling informed decision-making in smart agriculture.

Keywords IoT-based ammonia monitoring, LoRAWAN sensor network, Smart agriculture, GHG emission control, Agro-environmental decision support

Nitrogen fertilization is a widely used practice for enhancing agricultural crop production worldwide and is predicted to increase by 2050[1,2]. Nitrogen is an essential element for plant growth and agricultural production[3,4]. Although nitrogen is useful for plant nutrition, excessive and improper application can cause the loss of nitrogen via different mechanisms, including leaching (NO_3^-, NH_3^+, and organic N), volatilization (NO_x and NH_3), and gaseous forms (N_2O and NO) to the atmosphere[3,5]. Ammonia (NH_3) is not a greenhouse gas; however, once released to the atmosphere it contributes to $PM_{2.5}$ formation and to indirect N_2O emissions via the deposition of NH_4^+/NO_3^-[6]. The NH_3 emitted after fertilizer application is a major pathway of reactive nitrogen loss from cereal systems and a contributor to secondary particulate matter formation. Yet, high-frequency, in-field

[1]Albert Kázmér Mosonmagyaróvár Faculty of Agricultural and Food Sciences, Department of Biosystems Engineering and Precision Technology, Széchenyi István University, Mosonmagyaróvár, Hungary. [2]Department of Geography and Geoinformatics, The Islamia University of Bahawalpur, Bahawalpur 63100, Pakistan. [3]School of Natural Sciences, Botany Discipline, Trinity College Dublin, Dublin 2, Ireland. [4]Department of Physical Geography and Geoinformatics, Faculty of Science and Technology, University of Debrecen, Debrecen 4032, Hungary. [5]Institute of Land Use, Technical and Precision Technology, Faculty of Agricultural and Food Sciences and Environmental Management, University of Debrecen, 4032 Debrecen, Hungary. [6]Institutes for Agricultural Research and Educational Farm, University of Debrecen, Böszörményi 138, 4032 Debrecen, Hungary. [7]Department of Business Administration, Faculty of Business, Applied Science Private University, Amman, Jordan. ✉email: nyeki.aniko@sze.hu

observations remain rare because reference-grade instruments are costly and power-hungry, and telemetry in rural landscapes is challenging. Low-power sensing combined with LoRaWAN offers a practical alternative for continuous, near-surface NH_3 monitoring at the plot scale.

NH_3^+ emissions, primarily originating from agricultural activities, significantly impact up to 94% of global NH_3^+ emissions originate, of which 71% and 23% are from livestock production and fertilizer application, respectively[7]. Estimates show that the annual NH_3^+ emissions from manure and synthetic fertilizer are 3.79 Tg N and 12.32 Tg N respectively[8]. Livestock production and housing, vegetable production, fertilization practices, as well as manure and slurry management are the main sources of NH_3^+ emissions in the agricultural sector[9–11]. NH_3^+ emissions from agricultural activities not only reduce the efficiency of nitrogen but can also cause several detrimental effects such as soil acidification, air and water pollution, climate change, biodiversity loss, and damage to human health[9,11,12]. High nitrogen (N) fertilizer applications in conventional vegetable production systems lead to significant emissions of NH_3^+, which can cause haze pollution and ecosystem eutrophication[13]. The organo-mineral formulation decreased NH_3^+ losses by 50% and 90% in the dry and wet seasons, respectively. However, N_2O emissions increased by 91% in the wet season compared to the use of granular urea (UR) alone.

In addition, NH_3^+ emissions from agriculture are responsible for generating $PM_{2.5}$[14,15], exposure to which can cause chronic illnesses and increase the rate of mortality[16,17]. Furthermore, NH_3^+ is a precursor of pollutants, such as sulfur dioxide (SO_2) and nitrogen oxide (NO_x), and it has a significant impact on their formation[18,19]. In the agricultural sector, the emissions of NH_3^+ depend on several management and environmental factors, including meteorological, soil characteristics, manure composition, livestock species and their diet patterns, housing systems, synthetic fertilizer types and applications, and biomass burning[9,20].

Mitigation of NH_3^+ is crucial to achieve the purposes of improving environmental quality, cleaner production, and human health[11,21]. Strategic development management is necessary to mitigate NH_3^+ emissions, which requires reliable measurement methods and results in numerous health and environmental advantages[1,17,22]. In addition, accurate measurement of ammonia emissions from agricultural lands is necessary to improve agricultural fertilization practices, optimize nitrogen management, and increase its use efficiency[23,24]. Field ammonia emission measurements are difficult, so data on ammonia emissions and fluxes are largely unreliable[21]. Monitoring ammonia (NH_3^+) produced in agricultural fields is extremely important since it poses a huge threat to the environment. To optimize nitrogen management – especially in precision agriculture -, it is important to understand field ammonia emissions[21]. Several methods are available for measuring ammonia emissions from fields, including wind tunnels, chambers, portable ammonia detectors (PAD), and micrometeorological techniques[25–28]. Even though standard monitoring process relies on manual achievement and gas sensors face great challenges in the agricultural environment due to its complexity[29], but Meade et al.[26] suggest a micrometeorological technique for measuring ammonia emissions in the fields. Beyond high-cost micrometeorological techniques and chamber-based flux measurements, many national and regional networks still rely on passive diffusive samplers that provide monthly integrated NH_3 concentrations. For Europe, the EN 17346:2020[30] standard defines performance and handling requirements for such samplers, and well-established networks (e.g., the UK National Ammonia Monitoring Network) routinely operate on monthly exposure cycles[10]. While these approaches are valuable for spatial coverage and long-term trends, they cannot resolve short-lived emission peaks following fertilizer applications or rain events. Micrometeorological techniques offer high precision and accuracy, represent larger areas and field scales, and show lower spatial variability[31,32]. However, they are limited by high cost, the need for special analytical instruments, and expertise, which limit their broader application. Conversely, chamber-based methods are widely used because they are relatively inexpensive, and easier to install and operate[32]. Yet, static-chamber monitoring and portable devices remain time-consuming with limited field applicability and provide coarser temporal resolution. Since soil emission fluxes vary with meteorological, climatic, and agrotechnical conditions[33]. Therefore, automatic and continuous detection systems are more desirable in long-term field experiments[34]. Building on recent field evaluations, Molleman et al.[35] demonstrated that low-cost metal-oxide semiconductor sensors can quantify agricultural NH_3 at sub-ppm to ppm levels, provided that rigorous calibration, cross-sensitivity control, and environmental-drift correction are applied.

Precision agriculture uses Internet of Things (IoT) based monitoring system to monitor the environment and crop growth in real time, allowing for better planning and control of sustainable agriculture[36]. Using IoTs to collect environmental data is becoming increasingly regular in climate smart agriculture[37,38]. The IoT is connected through Wireless Sensor Networks (WSN), Radio-frequency Identification (RFID), Bluetooth, Near-field communication (NFC), Long Term Evolution (LTE), and many other smart communication technologies[39]. With Smart Farm Net IoT platform, data collection can be automated from various parameters related to agriculture, such as environmental parameters, fertilization, soil, irrigation, etc. IoT also provides tools to assess crop performance and construct crop forecasts by correlating data and removing invalid variables[40]. The integration of modern sensors with IoT in agriculture helps to monitor greenhouse gases (GHGs) like NH_3^+ emissions via automated sensors. This allows for better management of GHG emissions, which contributes to increased agricultural production and lower economic losses[24]. Complementing networked IoT approaches, Zhou et al. (2021)[23] demonstrated a membrane-permeation, conductometric probe for real-time, on-site monitoring of soil NH_3 flux in field deployments, illustrating the feasibility of high-temporal-resolution measurements but as single-deployment units rather than long-range, multi-node telemetry. Synthesizing evidence across agriculture and air-quality studies, Wyer et al. (2022)[41] conclude that ammonia emissions from agriculture are a major precursor of $PM_{2.5}$ with clear implications for human health, underscoring the need for high-temporal-resolution measurements around fertilization and manure-handling events.

Despite substantial research in monitoring NH_3 emissions, most of the existing approaches relied in chamber based or micrometeorological methods which are expensive, labor-intensive, and poorly suited for small scale spatially distributed field measurements. This lack leaves a clear gap in capturing short term

dynamics of agricultural NH_3 emissions under real field conditions. From this perspective, our study fills the gap by demonstrating open-field NH_3 monitoring at a 10-minute temporal resolution through field-deployable, LoRaWAN-connected NH_3 sensor network with integrated microclimate and soil sensors. The system explicitly captures multi seasonal agricultural NH_3 emissions, providing actionable insights into emission timing and magnitude. Hence, novelty of the work lies in practical adaptation of low-cost IoT technology to agricultural NH_3 monitoring, validated over multiple growing seasons. Specifically, we aimed (1) to efficiently utilize the LoRaWAN IoT system[42] to continuously monitor the NH_3 emissions together with environmental factors (air and soil temperature, rainfall, relative humidity, and soil moisture) in a wheat-barley cropping system from 2020 to 2023 at 10-minute temporal resolution; (2) to examine the yearly mean temporal differences between the variables and to characterize temporal patterns across seasonal and interannual scales; (3) to explore the dimensions and relationships among the variables and drivers of NH_3 using statistical analyses. The farm-based effective monitoring of real time ammonia emissions and its influencing environmental factors provides practical implications of sustainable site-specific farming practices which can lead to adopt climate smart agriculture.

Materials and methods

Study area and experimental design

To fulfil our hypotheses, the study was conducted from 2020 to 2023 under winter wheat and winter barley cultivation. The experimental field was located in Mosonmagyaróvár, Hungary [N47°54'20.00"; E17°15'10.00"] within Széchenyi István University (Fig. 1). The site covered an area of 23 hectares, with a gentle 5% slope and an elevation varying between 133 m and 138 m above sea level. According to the USDA classification system, the soil texture types of the agricultural field are loam, silty loam, and sandy loam. Field nodes were installed within cereal plots at 30 cm above the soil. The 30 cm height was chosen to characterize near-surface concentrations relevant to volatilization immediately above fertilized soil while minimizing crop damage. Sensors were oriented away from direct spray mounting minimized nearby surfaces that could affect gas adsorption.

During cereal harvest, stubble tillage is done mostly on fields with harrow and cultivator tillage, moldboard ploughing (~20 cm) and disking at the end of summer, and tooth harrowing for seedbed preparation. Spring cereals are ploughed in late fall and tillage systems are prepared in spring. The applied agrotechnology and tillage practices varied during the three full vegetation period (Table 1).

Fig. 1. Location of 23-ha experimental field sowing with winter wheat. Insets: photographs of the experimental field and sensor nodes taken by the authors. The map was created by the authors using ArcGIS Pro, version 3.2.0 (Esri Inc., Redlands, CA, USA; available at https://www.esri.com/en-us/arcgis/products/arcgis-pro/overview).

Tillage practices	2019/2020 – winter wheat	2020/2021 – winter barley	2021/2022 – winter wheat
Seedbed preparation and sowing	2019. 10. 25.	2020. 10.11.	2021.10.10–11.
Fertilizing hanging	2020.02.22. 56 kg N/ha	2021.02.24. 54 kg N/ha	2022.03.08. 38 kg N/ha
Fertilizing		2021.04.09. 31 kg N/ha	2022.04.02. 35 kg N/ha
Top dressing		2021.04.18. 4.4 l/ha	2022.05.22. 8 l/ha
Harvesting	2020.17-18.	2021.06.22-24.	2022.07.01-02.
Disking	2020.07.20.		
Gruber		2021.07.10.	2022.07.31.
Gruber		2021.08.15.	2022.09.02.
Gruber		2021.09.20	
Mouldboard plough	2020.09.10.		2022.09.20.
Digging	2020.10.05.	2021.10.09.	2022.10.15.

Table 1. Tillage practices and soil Preparation in the experimental field (2019–2022).

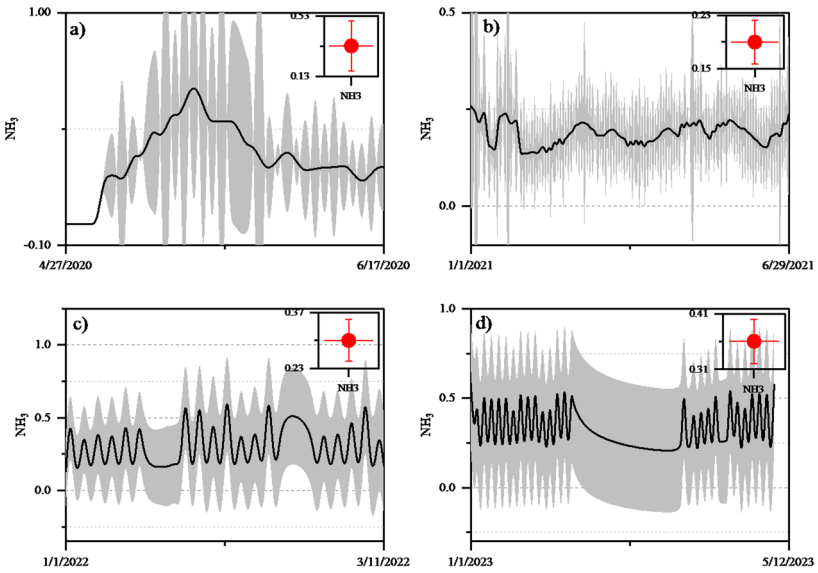

Fig. 2. Evolution of NH_3 emissions within the study field based on observed data between 2020 and 2023 (**a**) 2020, (**b**) 2021, (**c**) 2022, (**d**) 2023.

Cutting edge transmission technology for measuring NH_3 emissions

To meet the research objectives, a Field Monitoring Laboratory system[43,44] comprised of sensors and IoT technology was installed. The experimental site consisted of loam soil (44.2% sand, 12.5% clay, and 43.3% silt) with an organic matter content of 2.04% and a pH of 7.5. The field laboratory was equipped with soil, crops, and environmental (micro-meteorological) sensors, designed for real-time monitoring of agricultural conditions using the LoRaWAN communication protocol. The system comprised a field laboratory, a data server, and a self-developed dashboard and software for data analysis, visualization, and alert generation. The core objective was to automate data collection and enable remote monitoring of crops, soil, and environmental parameters in real time, accessible from any device at any location. A solar-powered sensor station was installed at a fixed GPS-referenced point in the field immediately after sowing and removed before crop harvest. Calibrated semiconductor gas sensor probes, operating with ultra-low power consumption (< 1 mA) and a measurement error below 1%, were positioned 30 cm above the soil surface to monitor near-surface ammonia (NH_3) concentrations. (Fig. 2b). In parallel with soil gas emissions, soil temperature and moisture content, air temperature, humidity and pressure values were also measured. (The BME280 is a digital temperature, humidity and pressure sensor developed by Bosch Sensor Tec.). NH_3 emissions were monitored using the Libelium Smart Environment Pro (SE-PRO 1) probe, an electrochemical ammonia gas sensor, a standard method with high selectivity for trace-level agricultural NH_3 monitoring. Ammonia gas sensor has a measuring rate between 0 to100 ppm (https://euro-gasman.com/media/wysiwyg/Gas_Sensors/SOLIDSENSE/4_NH3_100_1.pdf) with 0.135 +/- 0.035 µA/ppm sensitivity.

Meteorological and gas-emission data were acquired using an IoT-based environmental monitoring system. Air temperature and relative humidity were measured using a capacitive thermo-hygrometer (accuracy ± 0.5 °C and ± 3%, respectively). Soil temperature and volumetric soil moisture were measured using an in-soil thermistor probe (± 0.5 °C) and a capacitance-based soil moisture sensor (± 3%), respectively.

Data on emissions were collected at 10 min intervals, ensuring high temporal resolution for each day in crop growth season of wheat i.e., January to June. Data was preprocessed handling missing and outliers followed by averaging on daily basis for a more comprehensive analysis.

Sensor node and electronics
Each node integrates a low-power NH_3 sensor (0–100 ppm nominal measuring range) and an environmental sensor (temperature, relative humidity, pressure). Sampling was performed every 10 min with an internal averaging window to reduce short-term noise. Power was supplied by a rechargeable battery sized for multi-week operation; data were transmitted via a LoRaWAN Class A uplink on EU868 frequencies with Adaptive Data Rate (ADR); that confirmed uplinks are reserved for configuration to minimize energy use; and that a LoRaWAN network server manages session integrity and routes measurement payloads via MQTT into our time-stamped data pipeline.

Calibration and QA/QC
Calibration combined zero checks with scrubbed air and span checks with certified NH_3 standards bracketing the expected field range. Each sequence included sufficient stabilization at each step; pre- and post-deployment checks quantified drift. Temperature/relative-humidity compensation was derived from the co-located environmental measurements to mitigate humidity-dependent baseline shifts common to sensors. Routine bump tests in the field verified response. Data quality flags (e.g., missing packets, extreme values, calibration windows, failed bump tests) were recorded and propagated to analysis.

LoRaWAN networking and data pipeline
Nodes communicated with a nearby gateway and routed frames to a network/application server. Payloads were decoded on the application backend, stored in a time-series database, and visualized in a custom dashboard. The pipeline enforced automated quality-control rules (e.g., packet loss, range checks) and produced both 10-min data and daily aggregates for exploratory statistics (boxplots, pairwise comparisons, correlation, PCA).

Statistical analysis

The interplay between NH_3 emissions and meteorological variables was studied with a comprehensive statistical analysis. First, descriptive statistics including minimum, maximum, mean, standard deviation, range, and skewness were calculated on a basis for all selected variables from 2020 to 2023. The Tukey Kramer test was applied for a pairwise comparison between the means of all variables for each year. The Tukey test was employed after analysis of variance (ANOVA) to identify significant differences among various groups[45]. The test calculates a critical range, and if the difference between the two groups exceed this range, it is considered statistically significant ($p < 0.001$). The method balances comprehensive pairwise comparisons and controls the overall experiment-wise error rate[46]. Furthermore, Principal Component Analysis (PCA) was employed using a covariance matrix to identify components with maximum variance explained. PCA is a linear feature extraction method that captures significant variations along its orthogonal axes. For the current dataset, PCA is utilized to explore the significant dimensions of data structure to reveal the pattern and distribution across different years[47]. Principal components interpreted based on eigenvalues above 1 are used to unravel the complex and inherent pattern of data structure plotted in two dimensions. The varimax rotation method is adopted and eigenvectors determine the weight and direction of each component. Moreover, Spearman Correlation was employed to evaluate the monotonic relationship between variables using the ranks of the data, presented by the Eq. (1).

$$r_s = 1 - \frac{6\sum d_i^2}{n\left(n^2 - 1\right)} \tag{1}$$

Results

A statistical analysis of NH_3 emissions and environmental variables

Overall, NH_3 emissions and environmental data recorded by IoT sensors significantly varied from 2020 to 2023. The descriptive statistical analysis revealed notable temporal variations in the mean, minimum, maximum, and range of all variables (Table 2). Moreover, the seasonal emission trend depicted an increase in NH_3 emissions at the beginning of the growing season, where an accelerated increase of emissions is noticed. Then, the emission stabilizes for a certain period, as can be seen in the year 2020. However, more intense data were captured, showing a fluctuation in the emission. Nevertheless, the trend remains an increase at the beginning of the growing season as illustrated year-by-year in Fig. 2a (2020), Fig. 2b (2021), Fig. 2c (2022), and Fig. 2d (2023).

Following the descriptive analysis of all variables, the Tukey's pairwise comparisons revealed significant interannual variations among the studied variables across the years. For NH_3, a significant ($p < 0.05$) difference was observed between Y2022 vs. Y2020, Y2022 vs. Y2021, Y2023 vs. Y2020, and Y2023 vs. Y2021. Additionally, the maximum NH_3 emissions, reaching 1.94 ppm, are recorded in the year 2020 maintaining the highest range of 1.93 among all year's means. Subsequently, in 2021, the maximum emissions reached 1.7 ppm (Table 2). The smallest range of NH_3 emissions, at 0.5 ppm is observed in the year 2023, followed by 0.6 ppm in 2022 (Table 2 and Fig. 3A).

Temporal pattern of air temperature also exposed a significant mean difference in the selected years at study site. In the year 2020, the highest mean temperature recorded was 17 °C, exhibiting a significant ($p < 0.001$) variance from the temperatures recorded in 2021, 2022, and 2023 (Fig. 3B). These results are complemented by the descriptive statistics presented in Table 2, which details a mean air temperature of 10 °C in 2021, showcasing the highest range of 37 °C. Conversely, the year 2022 displays the lowest mean air temperature at 4.3 °C,

Var	Abbr	Year	Mean	SD	Range	Minimum	Maximum	Skewness	SE
Ammonia	NH_3 (ppm)	2020	0.33	0.60	1.93	0.003	1.94	1.93	0.33
		2021	0.19	0.24	1.71	0.0009	1.71	2.61	0.18
		2022	0.30	0.21	0.67	0.13	0.80	1.17	0.30
		2023	0.36	0.18	0.52	0.19	0.71	0.83	0.26
Air temp	T (°C)	2020	17.73	3.68	16.26	9.50	25.76	-0.16	0.33
		2021	10.55	8.72	37.09	-5.82	31.27	0.51	0.18
		2022	4.39	3.36	14.95	-2.21	12.74	0.25	0.30
		2023	8.05	5.79	23.42	-3.32	20.10	0.16	0.26
Relative humidity	RH %	2020	63.54	14.24	56.20	39.30	95.50	0.46	0.33
		2021	71.72	15.95	58.65	41.35	100.00	0.18	0.18
		2022	71.43	12.24	47.03	46.27	93.30	-0.36	0.30
		2023	77.92	15.53	53.60	46.33	99.93	-0.64	0.26
Rainfall	R (mm)	2020	0.40	1.47	9.00	0.00	9.00	4.85	0.33
		2021	0.48	2.57	31.60	0.00	31.60	10.43	0.18
		2022	0.09	0.31	1.80	0.00	1.80	4.08	0.30
		2023	0.00	0.00	0.00	0.00	0.00	0.00	0.26
Soil moisture 20 cm	SM-20 cm	2020	1.17	0.20	0.76	0.67	1.43	-0.95	0.33
		2021	0.58	0.07	0.37	0.40	0.77	-0.39	0.18
		2022	1.27	0.09	0.47	0.98	1.45	-2.28	0.30
		2023	6.47	4.22	14.54	2.46	17.00	0.83	0.26
Soil temperature 20 cm	ST-20 cm	2020	16.64	1.96	7.88	13.41	21.29	0.68	0.33
		2021	9.12	5.62	21.21	2.10	23.31	0.83	0.18
		2022	4.15	1.07	4.01	2.60	6.61	0.33	0.30
		2023	7.54	4.10	14.30	1.50	15.80	0.37	0.26
Soil moisture 40 cm	SM-40 cm	2020	0.80	0.08	0.43	0.66	1.09	0.86	0.33
		2021	0.94	0.10	0.48	0.70	1.18	0.05	0.18
		2022	1.24	0.06	0.20	1.10	1.30	-0.60	0.30
		2023	5.30	2.82	11.55	2.71	14.26	1.07	0.26
Soil temperature 40 cm	ST-40 cm	2020	15.41	1.64	5.95	13.17	19.12	0.81	0.33
		2021	9.13	4.71	17.81	3.40	21.21	0.86	0.18
		2022	4.56	0.93	3.51	3.15	6.66	0.32	0.30
		2023	7.76	3.55	12.48	2.43	14.90	0.38	0.26

Table 2. Descriptive statistics of NH_3 emissions and meteorological variables in selected years (2020–2023).

accompanied by the narrowest range of 14 °C. This discrepancy establishes a significant difference from the temperature profiles observed in other years. It is important to mention that the temperature differences are not necessarily driven by climate changes in the study area; instead, they reflect unequal measurement periods, as some years have longer records than others.

Furthermore, pairwise comparison for relative humidity also proved significant differences in different years (Fig. 3C and Table 2). The highest mean humidity of 77% was observed in the year 2023 with a range of 53% with a significant difference from Y2021. Also, a significant difference was recorded between Y2022 vs. Y2021 and Y2023 vs. Y2021, nonetheless, the rest of the years were similar with no significant differences. Furthermore, rainfall (Fig. 3D) displayed marked year-to-year variability, with 2020 and 2021 showing wetter conditions than 2022 and 2023, aligned with enhanced NH_3 release during 2020.

Moisture conditions at 20 cm and 40 cm of soil depth had significant differences in different years. Exceptionally high soil moisture was recorded in 2023 with a mean of 6.4% and 5.3% at two specific depths. Moreover, the highest statistical range of SM i.e., 14.5% at 20 cm and 11.5% at 40 cm also revealed a high difference in the minimum and maximum moisture percentage at two different depths. Interestingly, all years, except Y2021 vs. Y2020, recorded a significant difference (Fig. 3F,G). Similarly, soil temperature differed significantly at two depths (20 and 40 cm) across the studied years. The temporal pattern is like air temperature, with the highest means of 16 °C and 15 °C at 20 and 40 cm, respectively. Moreover, Tukey's test indicated significant mean differences across successive years up to 2023. The largest ranges were observed in 2021 (21.0 °C at 20 cm; 17.8 °C at 40 cm). Tukey's analysis at both depths showed the same pattern and yielded the same results. Significant pairwise differences were recorded for Y2021 vs. Y2020, Y2022 vs. Y2020, Y2022 vs. Y2021, Y2023 vs. Y2020, and Y2023 vs. Y2022; no significant difference was found for Y2023 vs. Y2021 (Fig. 3D,H, and Table 2). The findings highlight the sensitivity of soil-atmospheric NH_3 exchange to interannual climatic variability and soi hydrothermal characteristics.

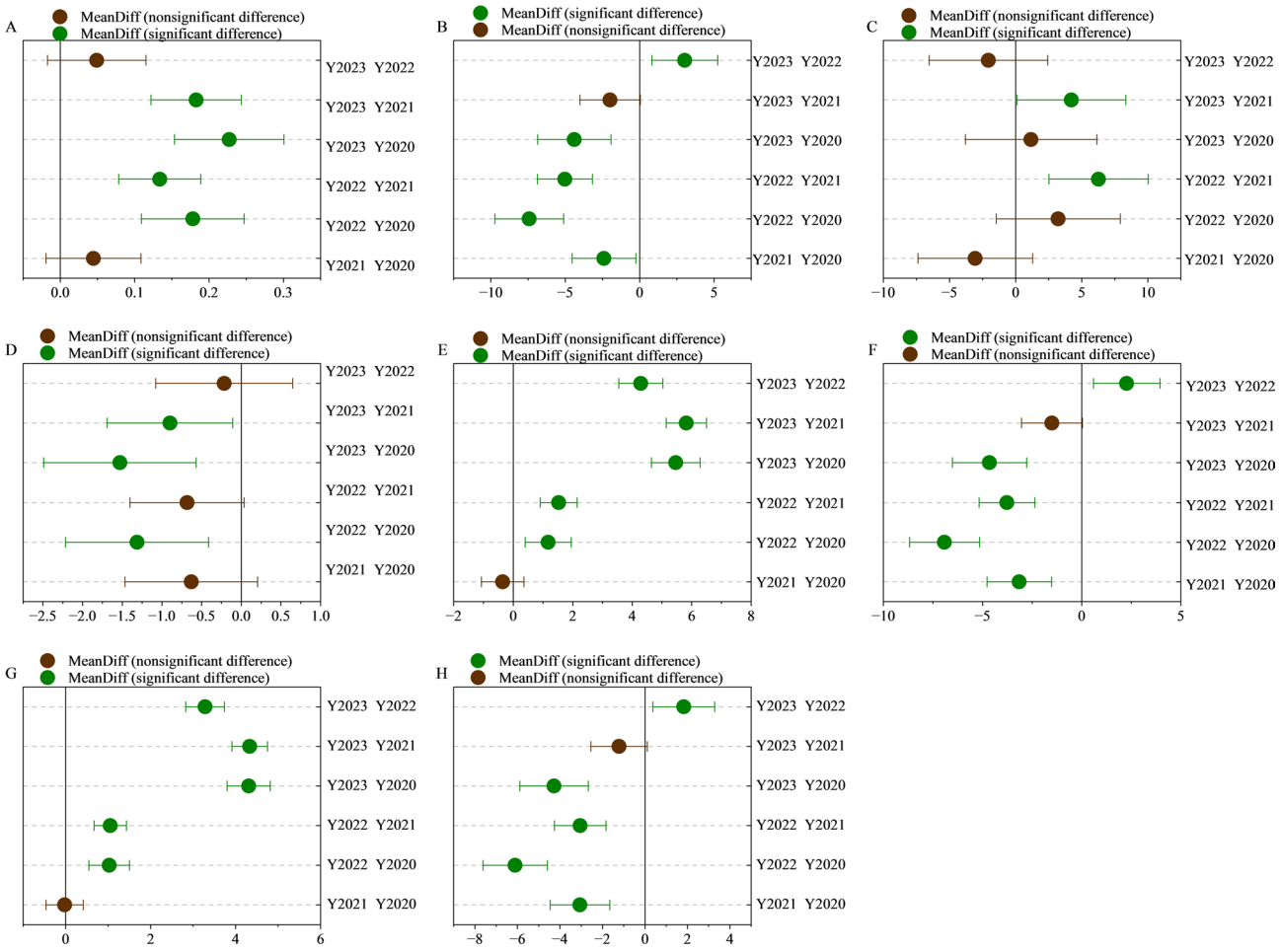

Fig. 3. Pairwise comparisons of mean of studied variables: (**A**) NH_3^+ emissions, (**B**) mean temperature (°C) emissions. (**C**) relative humidity (%), (**D**) rainfall (mm). (**E**) soil moisture (20 cm). (**F**) soil temperature (°C) (20 cm). (**G**) soil moisture (40 cm), (**H**) soil temperature (°C) (40 cm).

Spearman's correlation and principal component analysis

Spearman correlation of the variables revealed a positive significant correlation $r = 0.38$ to 0.4 of NH_3 with soil moisture at 20 cm and 40 cm of the soil depth. A stronger positive association was observed between soil moisture and soil temperature at both depths ($r > 0.7$), reflecting their coupled influence on soil atmospheric exchange. High significant correlations were observed between air temperature and soil temperature at 20 and 40 cm. On contrary, we found a negative correlation (r = -0.16 to -0.17) with soil temperature at 20 cm and 40 cm of soil depths which reveals the dynamics of NH_3 emissions (Fig. 4A,B). The year-to-year variability in NH_3, soil moisture (20 cm), and soil temperature (20 cm) is summarized in Fig. 4D–F. Overall, weak correlation of NH_3 with air temperature and rainfall suggested that short term fluxes are more strongly driven by microclimatic conditions rather than broader meteorological changes.

Furthermore, confidence ellipse revealed a temporal difference in the distribution pattern of environmental and soil variables (Fig. 4C). According to the analysis, 44% of the variability was explained by PC1 and 21.8% by PC2 (Table 3).

The biplot presents the distinct vector groups of variables with their loading effects on specific PCs. For example, air and soil temperature (°C) at different depths correlated with each other with the highest positive loading in PC1 with the coefficients of 0.47 and 0.48 (Table 4 and Fig. 4C). Contrary, soil moisture at 20 cm and 40 cm are correlated with each other with a high positive loading in PC2 with the coefficients of 0.60 and 0.59. Moreover, NH_3^+ has a more influence in PC2 with a coefficient loading of 0.22 less interrelated with meteorological variables while relative humidity suggests a least contribution captured by PC1 with a negative loading effect (Table 4 and Fig. 4C).

Discussion

Application of IoT in precision farming

The gaseous emissions of NH_3 from agriculture fields are detrimental for both land and environment causing loss of biodiversity and air pollution[41]. Ammonia volatilization due to fertilization causes environmental pollution from soil deposited ammonia with adverse environmental and health impacts[48]. For instance, Giannakis et al.[49]

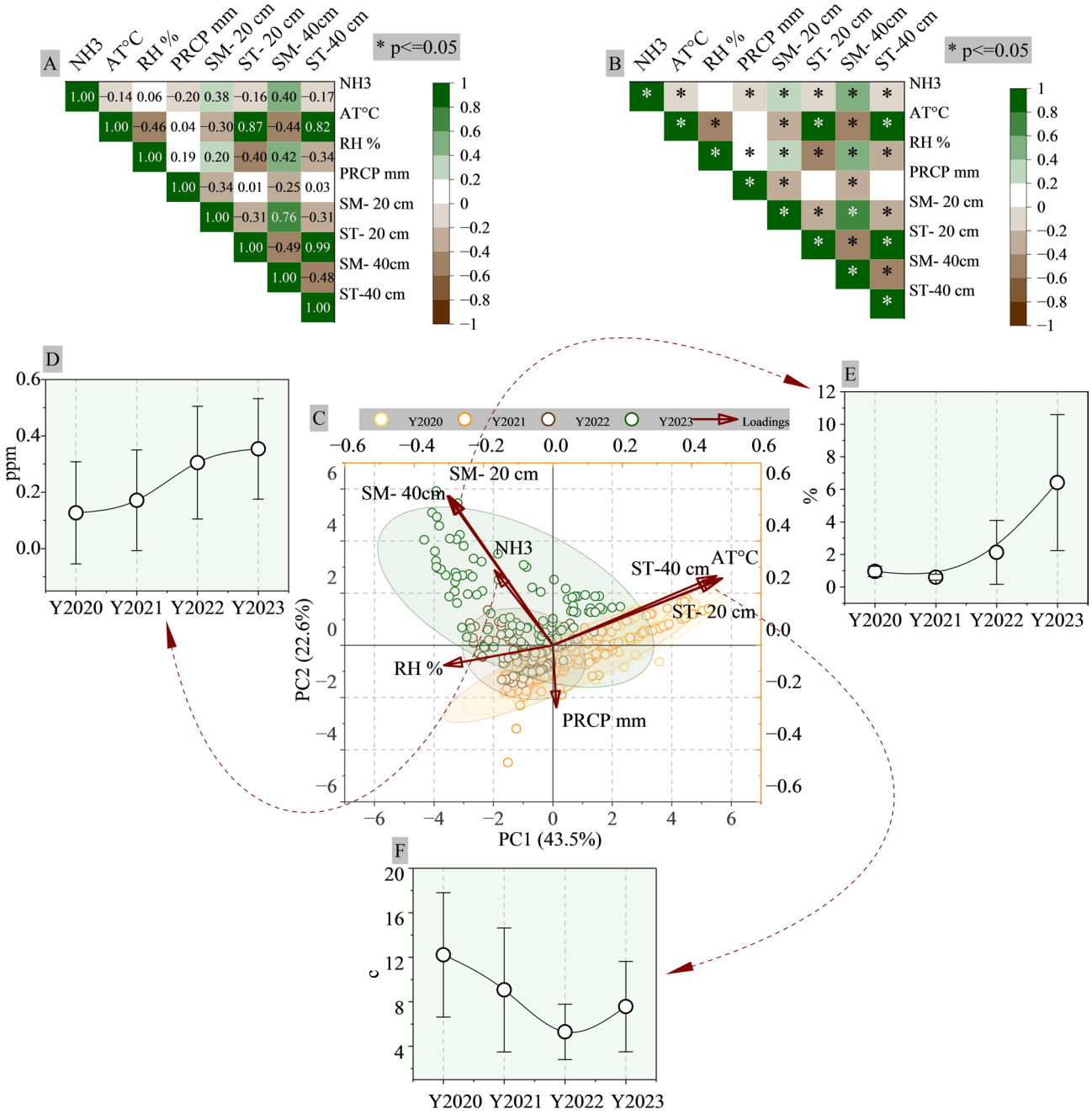

Fig. 4. Correlation matrix and principal component analysis for the studied dataset: (**A**, **B**) Sperman correlation between NH_3 and meteorological variables, (**C**) Biplot of principal components with 95% confidence ellipse, (**D**) mean and standard deviation for NH_3 data across years (2020–2023), (**E**) mean and standard deviation for soil moisture (20 cm) data across years (2020–2023), (**F**) mean and standard deviation for soil temperature (20 cm) data across years (2020–2023).

reported reported a high NH_3 emission in a few EU states with damaging impacts, NH_3 emissions contribute to air pollution, which can have implications for human health, ecosystems, and the environment. NH_3 emission causes eutrophication, toxic algal blooms, soil acidification, and nutrient imbalances. Hence, the role of IoT devices has become substantial in monitoring ammonia emissions at a farm scale level utilizing semiconductor-based sensors[50,51]. For example, ammonia gas sensors, predominantly utilizing semiconductor technologies, offer several advantages. Notably, Metal-Oxide Semiconductor (MOS) sensors and electrochemical sensors are widely employed in GHGs monitoring[35,52,53]. MOS sensors function by detecting alterations in electrical conductivity upon exposure to NH_3, providing sensitivity, cost-effectiveness, and suitability for continuous monitoring[54–56]. Their rapid responsiveness to changes in NH_3^+ concentration makes them particularly well-suited for real-time data acquisition in dynamic agricultural environments[35].

PCs	Eigenvalue	%age of variance	Cumulative
PC1	3.52	44.10%	44.10%
PC2	1.74	21.80%	65.91%
PC3	1.01	12.72%	78.63%
PC4	0.95	11.92%	90.55%
PC5	0.61	7.64%	98.18%
PC6	0.11	1.48%	99.66%
PC7	0.02	0.31%	99.97%
PC8	0.00	0.03%	100%

Table 3. Percent variance explained by principal components with eigenvalues.

Var	Coefficients PC1	Coefficients PC2
NH_3	-0.0448	0.228
T	0.478	0.247
RH	-0.355	0.0007
R	-0.026	-0.169
SM-20 cm	-0.296	0.605
ST-20 cm	0.483	0.260
SM-40 cm	-0.303	0.597
ST-40 cm	0.478	0.256

Table 4. Eigenvectors and coefficients of PC1 and PC2.

On the contrary, electrochemical sensors employ chemical reactions to generate electric current proportional to NH_3 concentration. Their durability and stability over extended periods ensure reliable, long-term data collection in agricultural settings[57,58]. The incorporation of these semiconductor sensors into IoT frameworks enhances their functionality. Linking these sensors to a network allows researchers to remotely monitor NH_3 emissions in real-time, enabling swift responses to environmental changes. This connectivity also streamlines data aggregation and analysis on a broader scale, contributing to a more comprehensive understanding of NH_3^+ dynamics in diverse agricultural landscapes[59]. This advanced technology not only facilitates farmers to optimize nitrogen fertilization but also enhances the environmental stewardship aligning the EU commitment of reducing GHG emissions for sustainable agricultural practices[59,60]. Recent developments in Wireless Sensor Network (WSN) technology have tailored the concept of smart farming. It comprises nodes with wireless communication capabilities, including sensors, converters, microcontrollers, and power sources facilitating the physical measurements of soil temperature and moisture content on agricultural fields[61,62]. Thus, the integration of IoT and WSN technology for monitoring ammonia emissions significantly contributes to big data analytics in precision agriculture empowering stakeholders with an insight for efficient and sustainable farming practices. Despite accurate farm monitoring of GHGs emissions from IoT sensors, the techniques are bound to the uncertainties arising from several factors such as calibration, environmental interference, sensor accuracy, and soil dynamics. Furthermore, data transmission errors in WSN should also be considered in accurate measuring of NH_3 emissions.

Temporal relationship of NH_3 emissions with meteorological variables

Ammonia is a highly reactive alkaline component released into the atmosphere as major agricultural emissions and considered to be the main contributors of aerosols development and largely affected by meteorological factors like temperature, humidity, and moisture conditions[63,64]. Hence, monitoring NH_3 emissions along with meteorological factors is crucial to examine the phenomenon and possible mitigation and soil management practices[65]. Oliveira et al.[66] studied the effects of organo-mineral formulation on crop yields, NH_3 volatilization, and N_2O emissions were evaluated in field experiments during dry and wet fertilization seasons. Findings of our study revealed that among various meteorological factors temperature and moisture play a key role in determining the rate of NH_3 emissions in varied agroclimatic conditions. As water saturation capacity of the soil decreases, NH_3 emissions from agricultural land increases[67]. Soil moisture and soil temperature affect the ammonia volatilization[68]. Our research findings revealed that NH_3 emissions in 2023 were the lowest (0.71 ppm) attributed to maximum soil moisture i.e., 17% and 14.26% at 20 cm and 40 cm of soil depth and negatively correlated with each other (Table 2). For instance, Han et al. (2014)[15] also explained that dried soil conditions trigger the large amount of NH_3 volatilization while irrigated soil helps to trap it in soil. Overall, average good soil moisture tends to facilitate soil microbial activities with favorable pH and soil temperature and enhance the transformation of soil nitrogen compounds. However, extreme soil moisture can also limit the oxygen availability in the soil due to water logging and hampers the microbial process which hinders the NH_3 emissions[69,70]. Parallel to soil moisture, soil temperature also plays a significant role in controlling NH_3^+ emissions in changing climatic scenarios. In particular, Butterbach-Bahl et al.[68] discussed the dynamics of NH_3 volatilization during spring

summertime of fertilization in future under high temperature and low soil moisture scenarios keeping several other factors as constant. High temperature directly impacts the NH_3 emissions by increasing hydrolysis of NH_4^+ to NH_3^+ and its diffusion into the atmosphere. Moreover, increased temperature also activates the soil urease during the decomposition of fertilizers and facilitates the whole process[71]. Hence, maximum ammonia emission of 1.94 ppm and 1.71 ppm in 2020 and 2021 is directly related to maximum high air temperature of 25 °C, and 31 °C and soil temperature of 21 °C and 23 °C in the respective years (Table 2). However, temperature alone does not facilitate the high NH_3 emissions but also supported by high rate of precipitation. Our findings also revealed that high ammonia emissions in the years 2020 and 2021 are associated with a high mean rainfall of 0.40 mm to 0.48 mm and maximum rain of 9 mm to 31.6 mm. (Table 2). It is supported by the study of[72] reporting that rain events soon after fertilization under high temperature conditions accelerates the soil microbial activity and enhances the NH_3^+ emissions. The observed phenomena are strongly influenced by the timing and quantity of fertilizer application, demonstrating the importance of optimized fertilization schedules[65,73]. Other than climatic factors, NH_3 volatilization also depends on soil texture with strong ammonium (NH_4^+) adsorption by clay soil leading water retention and less aeration[74] while high NH_3^+ emissions reported from loamy and sandy soil[75].

Measurements were single-point at 30 cm within the cereal canopy, which precludes resolving vertical gradients and field-scale heterogeneity following fertilization. The NH_3 sensor can exhibit humidity-dependent baselines and mild cross-sensitivities and adsorption, although compensation was applied, rapidly varying humidity may still introduce residual bias. Performance established under laboratory conditions can degrade in harsh field conditions; accordingly, we emphasize event detection and relative changes rather than absolute flux estimates. Future work will implement multi-height profiling and multi-point parallel sampling and will co-locate the Field Monitoring Laboratory with reference instrumentation to strengthen absolute accuracy.

Conclusions

This study demonstrates a LoRaWAN-based Field Monitoring Laboratory that delivers 10-minute, in-canopy, near-surface (30 cm) NH_3 observations suitable for long-term, farm-scale monitoring. The calibrated sensor, together with the end-to-end IoT pipeline (gateway → application/server → time-series storage → dashboard), provided robust data streams for statistical exploration. Inter-annual variability was confirmed by Tukey–Kramer tests. The analysis revealed that interannual crop seasonal climatic variability strongly influenced NH_3 emissions. Main statistical findings are concluded as; PCA demonstrated that NH_3 emissions were mainly driven by temperature-dependent volatilization, enhanced under moderately moist conditions, while high rainfall and humidity reduced emission intensity. A moderate positive correlation ($r = 0.38$ to 0.4) of NH_3 was observed with soil moisture at 20 cm and 40 cm of soil depth and weak negative correlation of -0.16 and −0.17 with soil temperature at 20 cm and 40 cm.

These findings are consistent with fertilization-driven, short-lived peaks captured at high temporal resolution. Because measurements were single-point at 30 cm, our interpretation prioritizes event detection and relative changes over absolute flux budgets. Known gas sensor characteristics (humidity-dependent baselines, mild cross-sensitivities) were mitigated by compensation and quality control. The system is implementable and reproducible for precision agriculture, and it underpins climate-smart nitrogen management. Future work will add multi-height profiling and multi-point parallel sampling and will co-locate the field node with reference instrumentation to improve absolute accuracy and generalizability.

Data availability

The datasets generated and/or analysed during the current study are available from the corresponding author on reasonable request.

Received: 1 October 2025; Accepted: 4 December 2025
Published online: 06 December 2025

References

1. Guo, Y. et al. Air quality, nitrogen use efficiency and food security in China are improved by cost-effective agricultural nitrogen management. *Nat. Food.* **1**, 648–658. https://doi.org/10.1038/s43016-020-00162-z (2020).
2. Lyu, X. et al. Reducing N2O emissions with enhanced efficiency nitrogen fertilizers (EENFs) in a high-yielding spring maize system. *Environ. Pollut.* **273**, 116422. https://doi.org/10.1016/j.envpol.2020.116422 (2021).
3. Pan, S-Y. et al. Addressing nitrogenous gases from croplands toward low-emission agriculture. *NPJ Clim. Atmos. Sci.* **5**, 43. https://doi.org/10.1038/s41612-022-00265-3 (2022).
4. Yu, X. et al. Global meta-analysis of nitrogen fertilizer use efficiency in rice, wheat and maize. *Agric. Ecosyst. Environ.* **338**, 108089. https://doi.org/10.1016/j.agee.2022.108089 (2022).
5. Rafique, R., Peichl, M., Hennessy, D. & Kiely, G. Evaluating management effects on nitrous oxide emissions from grasslands using the process-based DeNitrification–DeComposition (DNDC) model. *Atmos. Environ.* **45**, 6029–6039. https://doi.org/10.1016/j.atmosenv.2011.07.046 (2011).
6. Intergovernmental Panel on Climate Change (IPCC). *Refinement to the 2006 IPCC Guidelines for National Greenhouse Gas Inventories*. (2019).
7. Guthrie, S. et al. *The Impact of Ammonia Emissions from Agriculture on Biodiversity* (RAND Corporation and The Royal Society, 2018).
8. Ma, R. et al. Global soil-derived ammonia emissions from agricultural nitrogen fertilizer application: A refinement based on regional and crop-specific emission factors. *Glob Chang. Biol.* **27**, 855–867. https://doi.org/10.1111/gcb.15437 (2021).
9. Behera, S. N., Sharma, M., Aneja, V. P. & Balasubramanian, R. Ammonia in the atmosphere: a review on emission sources, atmospheric chemistry and deposition on terrestrial bodies. *Environ. Sci. Pollut. Res.* **20**, 8092–8131. https://doi.org/10.1007/s11356-013-2051-9 (2013).
10. Insausti, M., Timmis, R., Kinnersley, R. & Rufino, M. C. Advances in sensing ammonia from agricultural sources. *Sci. Total Environ.* **706**, 135124. https://doi.org/10.1016/j.scitotenv.2019.135124 (2020).

11. Ti, C., Xia, L., Chang, S. X. & Yan, X. Potential for mitigating global agricultural ammonia emission: A meta-analysis. *Environ. Pollut.* **245**, 141–148. https://doi.org/10.1016/j.envpol.2018.10.124 (2019).
12. Wang, H., Köbke, S. & Dittert, K. Use of Urease and nitrification inhibitors to reduce gaseous nitrogen emissions from fertilizers containing ammonium nitrate and Urea. *Glob Ecol. Conserv.* **22**, e00933. https://doi.org/10.1016/j.gecco.2020.e00933 (2020).
13. Wang, Y. et al. Characteristics of annual NH3 emissions from a conventional vegetable field under various nitrogen management strategies. *J. Environ. Manage.* **342**, 118276. https://doi.org/10.1016/j.jenvman.2023.118276 (2023).
14. Bauer, S. E., Tsigaridis, K. & Miller, R. Significant atmospheric aerosol pollution caused by world food cultivation. *Geophys. Res. Lett.* **43**, 5394–5400. https://doi.org/10.1002/2016GL068354 (2016).
15. Han, X. et al. Numerical analysis of the impact of agricultural emissions on PM 2.5 in China using a high-resolution ammonia emissions inventory. *Atmosph. Chem. Phys. Dis.* (2020).
16. Apte, J. S. et al. Ambient PM 2.5 reduces global and regional life expectancy. *Environ. Sci. Technol. Lett.* **5**, 546–551. https://doi.org/10.1021/acs.estlett.8b00360 (2018).
17. Lelieveld, J. et al. The contribution of outdoor air pollution sources to premature mortality on a global scale. *Nature* **525**, 367–371. https://doi.org/10.1038/nature15371 (2015).
18. Brunekreef, B. et al. Reducing the health effect of particles from agriculture. *Lancet Respir Med.* **3**, 831–832. https://doi.org/10.1016/S2213-2600(15)00413-0 (2015).
19. Thakrar, S. K. et al. Reducing mortality from air pollution in the united States by targeting specific emission sources. *Environ. Sci. Technol. Lett.* **7**, 639–645. https://doi.org/10.1021/acs.estlett.0c00424 (2020).
20. Hristov, A. N. et al. Review: ammonia emissions from dairy farms and beef feedlots. *Can. J. Anim. Sci.* **91**, 1–35. https://doi.org/10.4141/CJAS10034 (2011).
21. Yang, Y. et al. Measuring field ammonia emissions and canopy ammonia fluxes in agriculture using portable ammonia detector method. *J. Clean. Prod.* **216**, 542–551. https://doi.org/10.1016/j.jclepro.2018.12.109 (2019).
22. Plautz, J. Piercing the haze. *Sci. (1979).* **361**, 1060–1063. https://doi.org/10.1126/science.361.6407.1060 (2018).
23. Zhou, M. et al. Real-time on-site monitoring of soil ammonia emissions using membrane permeation-based sensing probe. *Environ. Pollut.* **289**, 117850. https://doi.org/10.1016/j.envpol.2021.117850 (2021).
24. Rajak, P., Ganguly, A., Adhikary, S. & Bhattacharya, S. Internet of things and smart sensors in agriculture: scopes and challenges. *J. Agric. Food Res.* **14**, 100776. https://doi.org/10.1016/j.jafr.2023.100776 (2023).
25. Gong, W., Zhang, Y., Huang, X. & Luan, S. High-resolution measurement of ammonia emissions from fertilization of vegetable and rice crops in the Pearl river delta Region, China. *Atmos. Environ.* **65**, 1–10. https://doi.org/10.1016/j.atmosenv.2012.08.027 (2013).
26. Meade, G. et al. Ammonia and nitrous oxide emissions following land application of high and low nitrogen pig manures to winter wheat at three growth stages. *Agric. Ecosyst. Environ.* **140**, 208–217. https://doi.org/10.1016/j.agee.2010.12.007 (2011).
27. Sekhar, P. K. & Kysar, J. S. An electrochemical ammonia sensor on paper substrate. *J. Electrochem. Soc.* **164**, B113–B117. https://doi.org/10.1149/2.0941704jes (2017).
28. Yang, Y. et al. Effects of conservation tillage practices on ammonia emissions from loess plateau rain-fed winter wheat fields. *Atmos. Environ.* **104**, 59–68. https://doi.org/10.1016/j.atmosenv.2015.01.007 (2015).
29. Li, X. et al. Toward agricultural ammonia volatilization monitoring: A flexible polyaniline/Ti3C2T hybrid sensitive films based gas sensor. *Sens. Actuators B Chem.* **316**, 128144. https://doi.org/10.1016/j.snb.2020.128144 (2020).
30. UKCEH. UKEAP 2022 annual report by UK Centre for Ecology and Hydrology: (2022).
31. Mosier, A. R. Gas flux measurement techniques with special reference to techniques suitable for measurements over large ecologically uniform areas. *Soils Greenhouse Effect* 289–301 (1990).
32. Zaman, M., Heng, L. & Müller, C. *Measuring Emission of Agricultural Greenhouse Gases and Developing Mitigation Options Using Nuclear and Related Techniques: Applications of Nuclear Techniques for GHGs* (Springer Nature, 2021).
33. Laville, P. et al. Effect of management, climate and soil conditions on N2O and NO emissions from an arable crop rotation using high Temporal resolution measurements. *Agric. Meteorol.* **151**, 228–240. https://doi.org/10.1016/j.agrformet.2010.10.008 (2011).
34. Minardi, I. et al. Evaluation of nitrous oxide emissions from vineyard soil: effect of organic fertilisation and tillage. *J. Clean. Prod.* **380**, 134557. https://doi.org/10.1016/j.jclepro.2022.134557 (2022).
35. Molleman, B. et al. Application of metal oxide semiconductor for detection of ammonia emissions from agricultural sources. *Sens. Biosensing Res.* **38**, 100541. https://doi.org/10.1016/j.sbsr.2022.100541 (2022).
36. Lin, N. et al. Fertigation management for sustainable precision agriculture based on internet of things. *J. Clean. Prod.* **277**, 124119. https://doi.org/10.1016/j.jclepro.2020.124119 (2020).
37. Ming, F. X., Habeeb, R. A. A., Md Nasaruddin, F. H. B. & Gani, A. Bin real-time carbon dioxide monitoring based on IoT & cloud technologies. In: *Proceedings of the 2019 8th International Conference on Software and Computer Applications*. 517–521 (2019).
38. Sinha, A., Shrivastava, G. & Kumar, P. Architecting user-centric internet of things for smart agriculture. *Sustainable Computing: Inf. Syst.* **23**, 88–102. https://doi.org/10.1016/j.suscom.2019.07.001 (2019).
39. Khanna, A. & Kaur, S. Evolution of internet of things (IoT) and its significant impact in the field of precision agriculture. *Comput. Electron. Agric.* **157**, 218–231. https://doi.org/10.1016/j.compag.2018.12.039 (2019).
40. Jayaraman, P. et al. Internet of things platform for smart farming: experiences and lessons learnt. *Sensors* **16**, 1884. https://doi.org/10.3390/s16111884 (2016).
41. Wyer, K. E. et al. Ammonia emissions from agriculture and their contribution to fine particulate matter: A review of implications for human health. *J. Environ. Manage.* **323**, 116285. https://doi.org/10.1016/j.jenvman.2022.116285 (2022).
42. LoRa. Technical Specifications. In: Lora Alliance. (Accessed 6 Nov 2025). https://resources.lora-alliance.org/technical-specifications. (2025).
43. Alahmad, T., Neményi, M. & Nyéki, A. Applying IoT sensors and big data to improve precision crop production: A review. *Agronomy* **13**, 2603. https://doi.org/10.3390/agronomy13102603 (2023).
44. Neményi, M. et al. Challenges of sustainable agricultural development with special regard to internet of things: survey. *Progress Agricultural Eng. Sci.* **18**, 95–114. https://doi.org/10.1556/446.2022.00053 (2022).
45. Cohen, A. L. *Problems and Pitfalls in Medical Literature: A Practical Guide for Clinicians* (Springer Nature, 2023).
46. Scherer, M. D. et al. Influence of postprocessing rinsing solutions and duration on flexural strength of aged and nonaged additively manufactured interim dental material. *J. Prosthet. Dent.* https://doi.org/10.1016/j.prosdent.2022.03.034 (2022).
47. Ringnér, M. What is principal component analysis? *Nat. Biotechnol.* **26**, 303–304. https://doi.org/10.1038/nbt0308-303 (2008).
48. van der Denier, H. & Bleeker, A. Indirect N2O emission due to atmospheric N deposition for the Netherlands. *Atmos. Environ.* **39**, 5827–5838. https://doi.org/10.1016/j.atmosenv.2005.06.019 (2005).
49. Giannakis, E., Kushta, J., Bruggeman, A. & Lelieveld, J. Costs and benefits of agricultural ammonia emission abatement options for compliance with European air quality regulations. *Environ. Sci. Eur.* **31**, 93. https://doi.org/10.1186/s12302-019-0275-0 (2019).
50. Al-Fuqaha, A. et al. Internet of things: A survey on enabling Technologies, Protocols, and applications. *IEEE Commun. Surv. Tutorials.* **17**, 2347–2376. https://doi.org/10.1109/COMST.2015.2444095 (2015).
51. Atzori, L., Iera, A. & Morabito, G. The internet of things: A survey. *Comput. Netw.* **54**, 2787–2805. https://doi.org/10.1016/j.comnet.2010.05.010 (2010).
52. Bruno, C. et al. Embedded artificial intelligence approach for gas recognition in smart agriculture applications using low cost MOX gas sensors. In: *2021 Smart Systems Integration (SSI)*. 1–5 (IEEE, 2021).
53. Gamal, Y. et al. IOT-based air quality monitoring system for agriculture. In: *2022 4th Novel Intelligent and Leading Emerging Sciences Conference (NILES)*. 206–210. (IEEE, 2022).

54. NAA, A., Kampara, R. K., R, P. K. & B.G. J Gold functionalized ZnO nanowires as a fast response/recovery ammonia sensor. *Appl. Surf. Sci.* **449**, 244–249. https://doi.org/10.1016/j.apsusc.2017.11.072 (2018).
55. Mhlongo, G. H. et al. A highly responsive NH3 sensor based on Pd-loaded ZnO nanoparticles prepared via a chemical precipitation approach. *Sci. Rep.* **9**, 9881. https://doi.org/10.1038/s41598-019-46247-z (2019).
56. Peng, R. et al. Reduced graphene oxide/SnO2@Au heterostructure for enhanced ammonia gas sensing. *Chem. Phys. Lett.* **737**, 136829. https://doi.org/10.1016/j.cplett.2019.136829 (2019).
57. Halley, S., Tsui, L. & Garzon, F. Combined mixed potential electrochemical sensors and artificial neural networks for the quantificationand identification of methane in natural gas emissions monitoring. *J. Electrochem. Soc.* **168**, 097506. https://doi.org/10.1149/1945-7111/ac2465 (2021).
58. Khan, M. A. et al. Recent trends in electrochemical detection of NH3, H2S and nox gases. *Int. J. Electrochem. Sci.* **12**, 1711–1733. https://doi.org/10.20964/2017.03.76 (2017).
59. Moysiadis, V., Sarigiannidis, P., Vitsas, V. & Khelifi, A. Smart farming in Europe. *Comput. Sci. Rev.* **39**, 100345. https://doi.org/10.1016/j.cosrev.2020.100345 (2021).
60. Soto, I. et al. *The Contribution of Precision Agriculture Technologies To Farm Productivity and the Mitigation of Greenhouse Gas Emissions in the EU* (Publications Office of the European Union Luxembourg, 2019).
61. Boursianis, A. D. et al. Internet of things (IoT) and agricultural unmanned aerial vehicles (UAVs) in smart farming: A comprehensive review. *Internet Things.* **18**, 100187. https://doi.org/10.1016/j.iot.2020.100187 (2022).
62. Ray, P. P. A survey on internet of things architectures. *J. King Saud Univ. - Comput. Inform. Sci.* **30**, 291–319. https://doi.org/10.1016/j.jksuci.2016.10.003 (2018).
63. Roelle, P. A. & Aneja, V. P. Characterization of ammonia emissions from soils in the upper coastal plain, North Carolina. *Atmos. Environ.* **36**, 1087–1097. https://doi.org/10.1016/S1352-2310(01)00355-7 (2002).
64. Skjøth, C. A. & Geels, C. The effect of climate and climate change on ammonia emissions in Europe. *Atmos. Chem. Phys.* **13**, 117–128. https://doi.org/10.5194/acp-13-117-2013 (2013).
65. Thies, S. et al. Fertilizer timing affects nitrous oxide, carbon dioxide, and ammonia emissions from soil. *Soil Sci. Soc. Am. J.* **84**, 115–130. https://doi.org/10.1002/saj2.20010 (2020).
66. Oliveira, B. G. et al. New trends in sugarcane fertilization: implications for NH3 volatilization, N2O emissions and crop yields. *J. Environ. Manage.* **342**, 118233. https://doi.org/10.1016/j.jenvman.2023.118233 (2023).
67. Yadav, S., Katoch, A., Singh, Y. & Kulshrestha, U. C. Abundance and variation of gaseous NH3 in relation with inorganic fertilizers and soil moisture during Kharif and Rabi season. *Environ. Monit. Assess.* **195**, 234. https://doi.org/10.1007/s10661-022-10777-3 (2023).
68. Butterbach-Bahl, K. & Dannenmann, M. Denitrification and associated soil N2O emissions due to agricultural activities in a changing climate. *Curr. Opin. Environ. Sustain.* **3**, 389–395. https://doi.org/10.1016/j.cosust.2011.08.004 (2011).
69. Abdul Rahman, N. S. N., Abdul Hamid, N. W. & Nadarajah, K. Effects of abiotic stress on soil Microbiome. *Int. J. Mol. Sci.* **22**, 9036. https://doi.org/10.3390/ijms22169036 (2021).
70. Martínez-Arias, C. et al. Beneficial and pathogenic plant-microbe interactions during flooding stress. *Plant. Cell. Environ.* **45**, 2875–2897. https://doi.org/10.1111/pce.14403 (2022).
71. Sha, Z. et al. Nitrogen stabilizers mitigate reactive N and greenhouse gas emissions from an arable soil in North China plain: field and laboratory investigation. *J. Clean. Prod.* **258**, 121025. https://doi.org/10.1016/j.jclepro.2020.121025 (2020).
72. Abdo, A. I. et al. Ammonia emission from staple crops in China as response to mitigation strategies and agronomic conditions: Meta-analytic study. *J. Clean. Prod.* **279**, 123835. https://doi.org/10.1016/j.jclepro.2020.123835 (2021).
73. Dubache, G. et al. Modeling ammonia volatilization following Urea application to winter cereal fields in the united Kingdom by a revised biogeochemical model. *Sci. Total Environ.* **660**, 1403–1418. https://doi.org/10.1016/j.scitotenv.2018.12.407 (2019).
74. Awale, R. & Chatterjee, A. Enhanced efficiency nitrogen products influence ammonia volatilization and nitrous oxide emission from two contrasting soils. *Agron. J.* **109**, 47–57. https://doi.org/10.2134/agronj2016.04.0219 (2017).
75. Panday, D. et al. Optimum rates of surface-applied coal Char decreased soil ammonia volatilization loss. *J. Environ. Qual.* **49**, 256–267. https://doi.org/10.1002/jeq2.20023 (2020).

Acknowledgements

The research was carried out by the "Precision Bioengineering Research GroupAnd by the János Bolyai Research Scholarship (Bo/00578/24) of the Hungarian Academy of Sciences. TKP2021-NKTA-32 has been implemented with the support provided by the Ministry of Culture and Innovation of Hungary from the National Research.

Author contributions

Anikó Nyéki: Writing—original draft, Methodology, Investigation, Formal analysis, Data curation, Conceptualization. Tarek Alahmad: Formal analysis, Data curation. Sana Arshad: Writing—original draft, Conceptualization. Nóra Gombkötő: Formal analysis, Data curation . Miklós Neményi: Investigation. Morad Mirzaei: Investigation, Formal analysis, Data curation.Szilárd Szabó: Investigation, Formal analysis. Endre Harsanyi: Data curation. Main Al-Dalahmeh: Investigation, Formal analysis, Data curation. Safwan Mohammed: Writing—original draft and reviewing, Methodology , Formal analysis, Visualization.

Declarations

Competing interests

The authors declare no competing interests.

Additional information

Correspondence and requests for materials should be addressed to N.A.